0026-895X/93/061267-11$03.00/0

MOLECULAR PHARMACOLOGY, 44:1267-1277



# Cytochrome P450 2B1-Mediated One-Electron Reduction of Adriamycin: A Study with Rat Liver Microsomes and Purified Enzymes

ARNOLD R. GOEPTAR, JOHAN M. TE KOPPELE, ELLEN K. LAMME, JUDITH M. PIQUÉ, and NICO P.E. VERMEULEN

*Leiden/Amsterdam Center for Drug Research, Division of Molecular Toxicology, Vrije Universiteit, De Boelelaan 1083, 1081 HV Amsterdam, The Netherlands*

Received June 15, 1993; Accepted September 17, 1993

**SUMMARY**

The role of cytochrome P450 (CYP) in the one-electron reductive bioactivation of Adriamycin (ADR) (doxorubicin) was investigated in subcellular fractions of the rat liver. The rate of one-electron reduction of ADR to its semiquinone free radical (ADRSQ), measured by ESR, was 5-fold greater with phenobarbital (PB)-induced (PB microsomes) than with β-naphthoflavone (βNF)-induced (βNF microsomes) rat liver microsomes under anaerobic conditions. ADRSQ formation was inhibited by SK&F 525-A and metyrapone (MP) in PB microsomes but was not significantly inhibited in βNF microsomes. Under aerobic conditions, the formation of ADRSQ from ADR was diminished in microsomal incubations and concomitant reduction of molecular oxygen occurred instead. Whereas ADR-induced $H_2O_2$ formation in PB microsomes was strongly inhibited by SK&F 525-A and MP, only a slight inhibition was observed with 2-ethynylnaphthalene and 1-ethynylpyrene in βNF microsomes. In addition, MP produced strong inhibition of ADR-stimulated lipid peroxidation in PB microsomes, compared with βNF microsomes. The idea that CYP2B1 was involved in the one-electron reduction of ADR in PB microsomes and in reconstituted systems of purified CYP2B1 and purified NADPH-CYP reductase (RED) under anaerobic conditions could be concluded from inhibition studies using SK&F 525-A and antibodies (KO1) against CYP2B enzymes. Moreover, it was calculated from reconstitution experiments using varying amounts of purified CYP2B1 and purified RED that the contribution of CYP2B1 to the one-electron reduction of ADR was similar to that of RED alone.

CYP, found in the endoplasmic reticulum of various organs and tissues, has the ability to metabolize a wide range of endogenous and exogenous compounds (1). RED, a FAD- and FMN-containing flavoprotein (2), plays a major role in the reduction of CYP during substrate oxygenation (1), oxidation (3), or reduction (4) reactions mediated by CYP. Particularly under anaerobic conditions, CYP has been shown to function in a reductive rather than an oxidative manner (4). Examples of substrate reduction include halogenated alkanes (5), triarylmethanes (6), nitro compounds (7), azo dyes (8), and NAPQIs (9). Preliminary evidence has also suggested the involvement of CYP in the reductive bioactivation of quinones such as danthron (10) and 1-piperidinoanthraquinone (11).

Quinones occur widely in nature and are clinically important in the treatment of a wide variety of tumors (12). An important quinone-containing anticancer drug used to treat human cancer is ADR (doxorubicin). ADR is an anthracycline type of antibiotic (for structure, see Fig. 10) exhibiting a broad spectrum of antitumor activities (12) but also cardiotoxicity (13) and nephrotoxicity (14). ADR is a typical redox cycling drug, i.e., a compound shuttling electrons from donor to acceptor molecules by virtue of its continuous reduction and reoxidation capability (15). The microsomal flavoprotein RED has been shown to catalyze the one-electron reduction of ADR to ADRSQ under anaerobic conditions (16). Under aerobic conditions, ADRSQ reoxidizes with concomitant formation of superoxide anion radicals ($O_2^{-\cdot}$) (17) and hydrogen peroxide ($H_2O_2$) (18). Prior investigations also suggested that redox cycling of ADR is mainly involved in the onset of toxicity (19). The toxicity of $O_2^{-\cdot}$ and $H_2O_2$ generated by redox cycling of ADR is probably mediated by iron through the formation of more potent oxidants, i.e., hydroxyl radicals (20–22). Hydroxyl radicals (·OH) can cause single-strand scissions of DNA (23) or initiate peroxidative lipid membrane decomposition (24, 25), a process leading to irreversible modifications of membrane structure and function (13).

**ABBREVIATIONS:** CYP, cytochrome P450; ADR, Adriamycin; ADRSQ, Adriamycin semiquinone free radical; βNF, β-naphthoflavone; DMPO, 5,5-dimethyl-1-pyrroline-*N*-oxide; DMU, dimethylureum; EN, 2-ethynylnaphthalene; EP, 1-ethynylpyrene; LPO, lipid peroxidation; MP, metyrapone; RED, NADPH-cytochrome P450 reductase; MMC, mitomycin C; TMQ, 2,3,5,6-tetramethylbenzoquinone; TMSQ, 2,3,5,6-tetramethylbenzoquinone semiquinone free radical; PB, phenobarbital; TBA, thiobarbituric acid; DTPA, diethylenetriaminepentaacetic acid; NAPQI, *N*-acetyl-*p*-benzoquinoneimine.

RED was first implicated as being involved in quinone reduction (16). However, CYP, which forms a part of the microsomal mixed-function oxidase system, has also been shown to participate in the reduction of the anticancer quinone MMC (25). In fact, the hepatic microsomal one-electron reduction of MMC has been shown to be inhibited by CYP inhibitors such as carbon monoxide, MP, and SK&F 525-A, suggesting that CYP itself is indeed responsible for quinone reduction (26). Both CYP2B1 (the major PB-inducible isoenzyme of CYP) (27) and RED were shown to be involved in the one-electron reduction of the model quinone TMQ to TMSQ under anaerobic conditions (28). Under aerobic conditions, CYP catalysis of TMQ-induced $H_2O_2$ formation, most likely due to redox cycling of the TMQ/TMSQ couple with molecular oxygen, has also been established by inhibition studies with SK&F 525-A (29).

Because quinones can undergo one-electron reductive bioactivation by CYP (25, 26, 28, 29) and because the toxicity and/or antitumor activity of quinone-containing cytostatic agents is mediated primarily by one-electron-mediated processes (21), it was considered of fundamental toxicological interest to elucidate further the mechanism of the one-electron reductive metabolism of ADR under both anaerobic and aerobic conditions, in a well defined *in vitro* system. The main objective of the present study was, therefore, to establish whether rat liver CYP is able to catalyze the one-electron reductive biotransformation of ADR and, if it is, to determine the relative contributions of CYP and RED in this one-electron reduction reaction. Also, an attempt was made to demonstrate that CYP-dependent reductive metabolism of ADR could lead to the formation of toxic reactive oxygen intermediates.

## Materials and Methods

**Animals.** Male Wistar rats (200–220 g; Harland-TNO, Zeist, The Netherlands) were housed in an environmentally controlled room (25°, 60% humidity), maintained on a standard laboratory diet (Hope Farms, Woerden, The Netherlands), and fasted overnight before use. The rats were pretreated with either sodium PB (100 mg/kg/day, in saline) or βNF (80 mg/kg/day, in arachid oil) by intraperitoneal injection for 3 or 2 days, respectively (30). Livers were isolated 24 hr after the last injection.

**Chemicals.** Glucose-6-phosphate, glucose-6-phosphate dehydrogenase, superoxide dismutase, NADP, glucose oxidase, catalase, cytochrome *c*, and NADPH were purchased from Boehringer (Mannheim, Germany). EDTA, semicarbazide, and formaldehyde were obtained from J.T. Baker (Deventer, The Netherlands). Butylhydroxytoluene, Tris·HCl, aminopyrine, and 7-ethoxyresorufin were from Sigma Chemical Co. (St. Louis, MO). TBA, resorufin, ascorbic acid, DMPO, and DMU were from E. Merck (Darmstadt, Germany). MP, DTPA, and βNF were obtained from Janssen Chimica (Beerse, Belgium). PB was from Brocacef (Maarssen, The Netherlands). ADR (Adriablastina, doxorubicin hydrochloride) was obtained from Farmitalia (Carlo Erba, Milan, Italy). SK&F 525-A (Proadiphen) was a gift of Smith Kline & French Laboratories (Helts, UK). EN and EP were kindly provided by Dr. W. L. Alworth (Tulane University, New Orleans, LA).

**Preparation of microsomes and enzyme purification.** Rat liver microsomes were prepared as described by Jefcoate (31) and were stored in liquid nitrogen until used. CYP2B1 was purified from livers of PB-induced rats, as described previously (32). Isolated and purified CYP2B1 was active in reconstituted systems, as shown by aminopyrine *N*-demethylation (55 nmol of HCHO/nmol of CYP2B1/min). CYP content was measured as described by Omura and Sato (33). RED was purified from PB-induced rat liver microsomes according to the method of Guengerich and Martin (32). RED activity was determined by its ability to reduce cytochrome *c* (34). RED concentration was determined fluorometrically according to the method of Faeder and Siegel (35), by measuring the flavin composition. Purified RED contained nearly equal amounts of FMN and FAD, with a molar ratio of FMN to FAD of 0.95, as shown previously (2). Protein was determined by the method of Lowry *et al.* (36), with bovine serum albumin as the standard.

**Difference spectrophotometry.** Interactions between ADR and microsomal CYP were studied by difference spectrophotometry, as described previously (28). Double-tandem cuvettes were used to correct for the intrinsic absorbance of ADR. Microsomes were diluted to 1 mg/ml protein in 100 mM Tris·HCl buffer, pH 7.4, containing 0.1 mM EDTA. ADR was dissolved in the same Tris·HCl buffer. The binding spectra were recorded on an Aminco DW 2a UV/visible spectrophotometer at room temperature (25°).

**Aminopyrine *N*-demethylation.** *N*-Demethylation of aminopyrine in PB-induced rat liver microsomes was measured as described elsewhere (29), with minor modifications. Briefly, the incubation mixtures consisted of 5 mM glucose-6-phosphate, 1 unit/ml glucose-6-phosphate dehydrogenase, 5 mM $MgCl_2$, 5 mM semicarbazide hydrochloride, 2.5 mM aminopyrine, 0–50 μM ADR, and microsomes (1 mg/ml protein), in 50 mM Tris·HCl buffer, pH 7.4. Incubation mixtures were equilibrated at 37° for 5 min. The *N*-demethylation reaction was started by the addition of 0.5 mM NADP and was carried out for 10 min. The rate of *N*-demethylation was determined as the amount of formaldehyde formed during 10 min of incubation and was measured according to the method of Nash (37), using a Philips PU-8720 UV/visible spectrophotometer (absorbance measured at 412 nm).

**7-Ethoxyresorufin *O*-deethylation.** *O*-Dealkylation of 7-ethoxyresorufin in βNF-induced microsomes was measured as follows. The incubation mixture (total volume, 1 ml) consisted of 22.7 μg/ml protein, 0.2 μM 7-ethoxyresorufin (dissolved in dimethylsulfoxide), and 0–50 μM ADR, in 50 mM Tris·HCl buffer, pH 7.4. The reaction was started by the addition of 0.5 mM NADPH, and resorufin formation was followed spectrofluorometrically for 2 min. The final incubation mixture contained 0.1% (v/v) dimethylsulfoxide, and at this concentration no effect on the 7-ethoxyresorufin *O*-deethylation activity was observed. The initial rate of deethylation was determined using a Perkin Elmer model 3000 spectrofluorometer (excitation and emission monochromators set to 535 and 582 nm, respectively).

**Hydrogen peroxide formation.** ADR-induced $H_2O_2$ production under aerobic conditions was measured in 1.0-ml incubation mixtures containing 1 mg/ml microsomal protein, 5.0 mM $MgCl_2$, 3000 mU of catalase, 5 mM semicarbazide, 50 mM methanol, 5 mM glucose-6-phosphate, and 1 unit/ml glucose-6-phosphate dehydrogenase, in 50 mM Tris·HCl buffer, pH 7.4. DTPA was added to a final concentration of 0.1 mM, to prevent nonspecific decomposition of $H_2O_2$. After 5 min of preincubation at 37° the reaction was started by the addition of 0.5 mM NADP, and it was stopped 10 min later by the addition of 0.5 ml of 20% trichloroacetic acid. $H_2O_2$ formation was determined as described previously (29), by measuring formaldehyde formed via the peroxidatic reaction of catalase in the presence of 50 mM methanol (38), and was measured according to the method of Nash (37).

**ESR measurements under anaerobic conditions.** One-electron reduction of ADR by rat liver microsomes was assayed by ESR in incubation mixtures consisting of 1 mg/ml microsomal protein, 0.1 mM ADR, 1 mM NADPH, 7.5 mM glucose-6-phosphate, 1 unit/ml glucose-6-phosphate dehydrogenase, and 50 mM phosphate buffer, pH 7.4, containing 0.5 mM DTPA. For ESR measurements in reconstituted systems of CYP2B1 and RED, equimolar concentrations (70 nM) of the two enzymes were mixed with dilauroylphosphatidylcholine (40 μg/ml). The composition of the reaction mixture was the same as described for the microsomal incubation. Anaerobic conditions were obtained by flushing the incubation mixtures, in sealed tubes, with argon gas before initiation of the reaction with NADPH (39).

**ESR measurements under aerobic conditions.** Stimulation by ADR (0.1 mM) of $O_2^{\cdot-}$ and $^{\cdot}OH$ formation was measured as described previously for TMQ (29), using DMPO (100 mM) as spin trap. Micro-

somal and purified enzyme preparations were kept on ice until used. The incubations were carried out at room temperature and the ESR spectra were recorded immediately after the initiation of the enzymic reaction, in an ESR quartz flat cell mounted in a cavity with a nominal microwave power of 25 mW and microwave frequency of 9.79 GHz. ESR measurements were performed with a Bruker ESP-300 spectrophotometer/ESP 1600 data processor. Incubation conditions and ESR parameters are indicated in the figure legends.

**Measurement of ADR-induced NADPH oxidation.** The initial rate of ADR reduction under anaerobic conditions in rat liver microsomes and in reconstituted systems of purified CYP2B1 and RED was measured by determining NADPH oxidation at 340 nm (using an extinction coefficient of 6.22 $mM^{-1}$ $cm^{-1}$) (40). The incubation mixture contained 50 mM Tris·HCl buffer, pH 7.4, 5 mM $MgCl_2$, and 0.5 mM DTPA, with microsomal protein (0.7 mg/ml), in a final volume of 1.0 ml at 37°. For the preparation of the reconstituted systems, CYP2B1 and RED were mixed with dilauroylphosphatidylcholine (40 μg/ml) as described above. ADR (final concentration, 0.1 mM) was added before the addition of NADPH (final concentration, 1 mM). Anaerobic incubations were carried out in sealed cuvettes, which were flushed with argon before temperature equilibration (39). In addition, traces of oxygen were removed from the incubation mixtures with 7.5 mM glucose, 13 units/ml glucose oxidase, and 1590 units/ml catalase, as described previously (39).

**ADR-induced LPO.** Rat liver microsomes were diluted 5-fold with ice-cold 50 mM Tris·HCl buffer, pH 7.4, containing 150 mM KCl, and were washed twice (centrifugation at 100,000 × *g* for 40 min at 4°). The pellets were resuspended in the same Tris·HCl buffer. The microsomes (1 mg/ml protein) were then incubated with ADR (0.1 mM), NADP (0.1 mM), and an NADPH-generating system of 1 unit/ml glucose-6-phosphate dehydrogenase and 5 mM glucose-6-phosphate, at 37° under a carbogen atmosphere (95% $O_2$/5% $CO_2$).

LPO was assayed as described by Haenen and Bast (41), by measuring TBA-reactive material. Briefly, a 0.3-ml aliquot of the incubation mixture was added to 2 ml of ice-cold TBA/trichloroacetic acid/HCl/butylhydroxytoluene solution. After heating for 15 min at 80° and centrifugation for 15 min at 4°, the absorbance at 535 nm versus 600 nm was determined in the supernatant. Corrections were made for the absorbance produced by ADR.

**Statistical evaluation of the data.** Data are presented as means ± standard deviations of at least three determinations, unless otherwise stated. Statistical evaluation of the data was performed with Student's *t* test. Differences were considered statistically significant at $p < 0.05$.

## Results

**Interaction between ADR and rat liver CYP.** The binding of ADR to PB- and βNF-induced microsomes was first determined by difference spectrophotometry. With PB-induced rat liver microsomes (PB microsomes) the ADR-induced difference spectrum of CYP showed a minimum at 397 and a maximum at 429 nm, indicating either a type II or a reverse type I interaction (Fig. 1). The spectral dissociation constant $K_s$ and $\Delta A_{max}$, calculated from the respective $1/\Delta A$ versus 1/[ADR] plots, were 1.14 ± 0.03 μM and 0.013 ± 0.002 AU/nmol of CYP (three experiments), respectively. To delineate the nature of the interaction between ADR and CYP in PB microsomes, the effect of ADR on the spectral changes induced by imidazole, a type II binding model substrate (42), was investigated. Up to 5 μM, ADR had no effect on the $K_s$ (104 μM) or $\Delta A_{max}$ (0.015 AU/nmol of CYP) of imidazole in PB microsomes, indicating that direct binding of ADR to the heme iron of oxidized CYP is not likely. In addition, ADR did not displace carbon monoxide from its binding site on the heme iron of sodium dithionite-reduced CYP (0.110 AU/mg of protein) in PB microsomes, as measured by difference spectrophotometry.

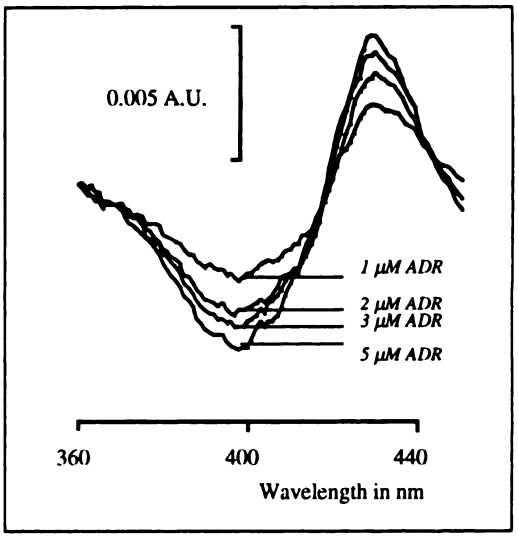


**Fig. 1.** Spectrophotometrically obtained difference spectra of the interaction between ADR and microsomal CYP. Binding spectra of ADR (1–5 μM) with PB-induced rat liver microsomes were obtained as described in Materials and Methods. Representative experiments of three are shown.

Both observations suggest a reverse type I interaction between ADR and PB-inducible CYPs. With βNF-induced rat liver microsomes (βNF microsomes), ADR failed to produce a difference spectrum, indicating a lack of interaction between ADR and βNF-inducible CYPs.

**Inhibition by ADR of CYP-dependent monooxygenase activities.** The interaction between ADR and rat liver CYP was further substantiated by determining the effect of ADR on the rate of metabolism of specific model substrates for CYP. ADR strongly inhibited the *N*-demethylation of aminopyrine in PB microsomes, in a concentration-dependent manner (Fig. 2). In contrast to PB microsomes, ADR did not inhibit the dealkylation of 7-ethoxyresorufin in βNF microsomes (Fig. 2). The rate of *O*-dealkylation was not affected by ADR even at concentrations up to 50 μM (Fig. 2). This observation is consistent with the lack of binding of ADR to βNF-inducible CYPs in βNF microsomes.

The fact that RED activity in these microsomal incubations, measured by its capacity to reduce cytochrome *c*, was not inhibited by ADR (1.44 ± 0.05 versus 1.45 ± 0.04 units/ml in the absence and presence of 0.1 mM ADR, respectively; four experiments) indicates that the site of inhibition of aminopyrine *N*-demethylation is CYP and not the flavoprotein RED. Inhibition of CYP by an ADR-derived metabolite could also be excluded, because no CYP-intermediate complex was detected spectrophotometrically upon prior incubation of PB microsomes with ADR and NADPH (data not shown).

The observed inhibitory effect of ADR on the CYP-mediated *N*-dealkylation of aminopyrine in PB microsomes may indicate competition between ADR and aminopyrine at the catalytic site of CYP. However, one may argue that the linear inhibition of aminopyrine *N*-demethylation by ADR, as indicated in Fig. 2, is not a very characteristic concentration curve, especially because saturation of the binding of ADR to PB microsomes was observed (Fig. 1). Therefore, we cannot rule out other interactions between ADR and CYP in PB microsomes.

**Formation of ADRSQ from ADR by CYP.** Anaerobic incubation of 0.1 mM ADR with PB microsomes in the presence

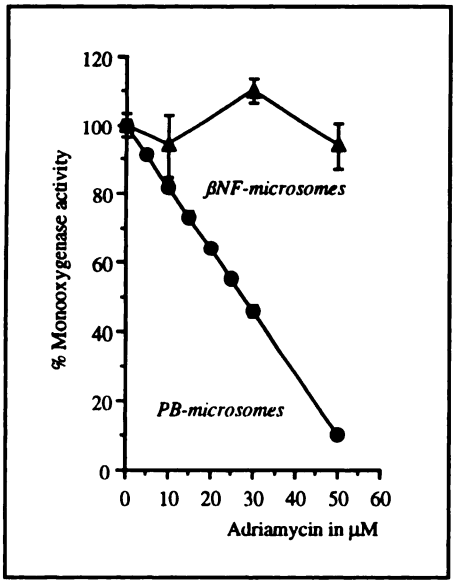


**Fig. 2.** Inhibition by ADR of CYP-dependent monooxygenase activities. The effect of increasing concentrations of ADR on the CYP-mediated dealkylation of aminopyrine in PB-induced rat liver microsomes (●) and of 7-ethoxyresorufin in βNF-induced rat liver microsomes (▲) was investigated as described in Materials and Methods. The 100% values in PB- and βNF-induced microsomes were 4.7 nmol of HCHO/nmol of CYP/min and 17.6 nmol of resorufin/nmol of CYP/min, respectively. The means ± standard deviations of three experiments are shown.

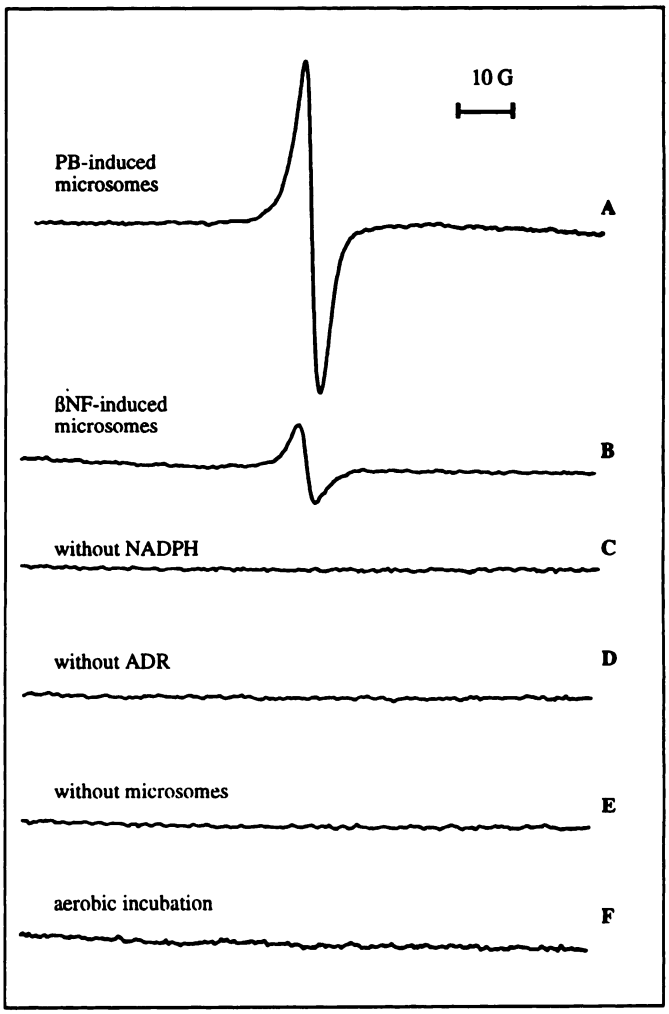


**Fig. 3.** ESR spectra of ADRSQ. ESR spectra were obtained upon anaerobic incubation of ADR with PB-induced microsomes (*spectrum A*) or βNF-induced microsomes (*spectrum B*). In control incubations without NADPH (*spectrum C*), without ADR (*spectrum D*), or without microsomes (*spectrum E*), no ESR signal was obtained. Under aerobic conditions (*spectrum F*) the ESR signal for ADRSQ disappeared completely. The ESR settings were as follows: microwave power, 25 mW; microwave frequency, 9.79 GHz; midfield, set at 3480 G; time constant, 655.36 msec; modulation frequency, 100 kHz; modulation amplitude, 1 G; receiver gain, $5 \times 10^5$; sweep width, 100 G; resolution, 1024 points; conversion time, 163.84 msec; number of scans, 10. Representative experiments of at least three are shown.

of a NADPH-generating system showed strong ESR signals for ADRSQ (Fig. 3, *spectrum A*). The ESR spectrum obtained was similar to that reported for ADRSQ by Kalyanaraman *et al.* (22). With βNF microsomes a 5-fold smaller ESR signal for ADRSQ was obtained under identical conditions (Fig. 3, *spectrum B*). Under aerobic conditions, the ESR signal for ADRSQ disappeared completely (Fig. 3, *spectrum F*), either due to redox cycling of ADRSQ with molecular oxygen (17, 18) or due to ADR-induced uncoupling of the CYP reaction cycle. When either NADPH, ADR, or PB microsomes were omitted, no ESR signal for ADRSQ could be detected in the microsomal incubations under anaerobic conditions (Fig. 3, *spectra C, D,* and *E*, respectively).

The effects of SK&F 525-A and MP, potent inhibitors of CYP (43), were also investigated to substantiate the role of CYP in the one-electron reduction of ADR (0.1 mM) to ADRSQ under anaerobic conditions. SK&F 525-A (1.0 mM) and MP (1.0 mM) strongly inhibited ADRSQ formation in PB-induced microsomes, as judged from the corresponding ESR signals for ADRSQ (Fig. 4, *spectra B* and *C* versus *spectrum A*). Because the ADRSQ concentration was stable under anaerobic conditions, the intensity of the ESR signal was used to quantify the amount of ADRSQ in the different microsomal incubations (Table 1). As expected, ADRSQ formation in PB microsomes was inhibited in the presence of SK&F 525-A and MP (Fig. 4; Table 1). These CYP inhibitors also inhibited ADRSQ formation in βNF microsomes (Table 1), but not statistically significantly (four experiments). At the concentrations used, SK&F 525-A and MP were not inhibitory to purified RED, as measured by cytochrome *c* reduction, nor did they affect the direct one-electron reduction of ADR by purified RED alone, as measured by ESR under anaerobic conditions (Table 1).

**ADR-induced molecular oxygen reduction in rat liver microsomes.** Compared with anaerobic conditions (Fig. 3, *spectrum A*), under aerobic conditions the ADRSQ formation in microsomal incubations was diminished (Fig. 3, *spectrum F* versus *spectrum A*). In the presence of DMPO, a DMPO-OOH radical was observed under aerobic conditions (Fig. 5, *spectrum A*), similar to that reported for the superoxide anion radical adduct of DMPO (44). Superoxide anion radicals ($O_2^{-\cdot}$) can dismutate to produce hydrogen peroxide ($H_2O_2$), which can be measured spectrophotometrically (38). In contrast to what was expected from the ESR measurement under anaerobic conditions (Fig. 3), ADR was able to induce $H_2O_2$ formation in both PB and βNF microsomes in a concentration- and time-dependent manner under aerobic conditions (Fig. 6). The endogenous $H_2O_2$ formation was 17.1 nmol of $H_2O_2$/nmol of CYP/min in PB microsomes and 4.5 nmol of $H_2O_2$/nmol of CYP/min in βNF microsomes. The $K_m$ and $V_{max}$ values for ADR-induced $H_2O_2$ formation (corrected for endogenous $H_2O_2$ formation) in

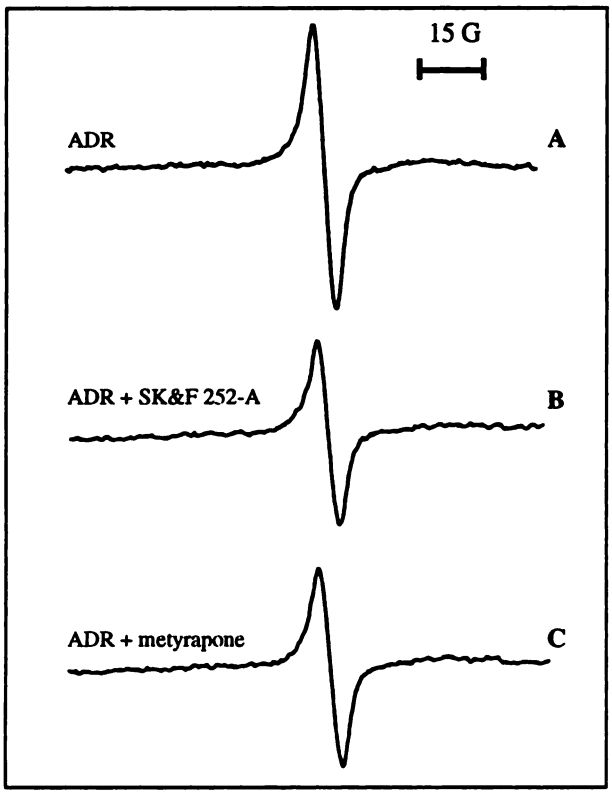


Fig. 4. Inhibitory effects of MP and SK&F 525-A on ADRSQ formation in PB-induced microsomes. ESR spectra were obtained upon anaerobic incubation of ADR (*spectrum A*) with either 1 mM SK&F 525-A (*spectrum B*) or 1 mM MP (*spectrum C*), as described in Materials and Methods. ESR settings were the same as described in the legend to Fig. 3. Representative experiments of four are shown.

TABLE 1

**Inhibition of the anaerobic microsomal one-electron reduction of ADR to ADRSQ by the CYP inhibitors SK&F 525-A and MP**

Peak areas were calculated by double-integration of the ESR signal for ADRSQ and are expressed as percentage of the maximal signal intensity. The means ± standard deviations of four experiments are shown.

| System | ADRSQ formation | | |
|---|---|---|---|
| | PB microsomes | βNF microsomes | Purified RED |
| | % | | |
| Complete[a] | 100 ± 18 | 15 ± 6 | 56 ± 6 |
| With SK&F 525-A (1 mM) | 41 ± 12[b] | 9 ± 5[c] | 50 ± 10[c] |
| With MP (1 mM) | 40 ± 17[b] | 8 ± 4[c] | 57 ± 8[c] |

Complete systems contained microsomes (1 mg/ml protein). The purified system contained 70 nM RED instead of microsomes. For experimental details, see Materials and Methods and the legend to Fig. 3.

[b] $p < 0.001$.

[c] Not significant.

PB microsomes were 0.9 mM and 0.111 μmol of $H_2O_2$/nmol of CYP/min, respectively. $K_m$ and $V_{max}$ values obtained in βNF microsomes were 0.6 mM and 0.07 μmol of $H_2O_2$/nmol of CYP/min, respectively.

Interestingly, SK&F 525-A completely inhibited ADR-induced $H_2O_2$ formation in PB microsomes, as did MP (a potent inhibitor of PB-inducible CYPs) (43) (Fig. 7A). However, SK&F 525-A was rather ineffective in inhibiting ADR-induced $H_2O_2$ formation in βNF microsomes (Fig. 7B). Moreover, EN (10 μM) and EP (10 μM), known suicidal inhibitors of βNF-inducible CYPs (45, 46), were only slightly inhibitory (from 100 ± 2% to 76 ± 4% and 71 ± 7%, respectively; three experiments; $p < 0.001$) in βNF microsomes. Importantly, these CYP inhibitors were shown neither to interfere with the $H_2O_2$ assay nor to affect RED activity (29).

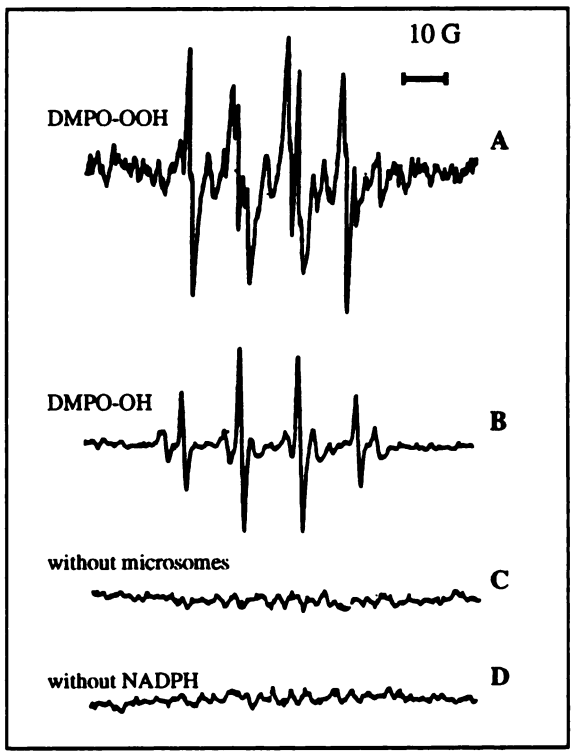


Fig. 5. Detection of ADR-induced DMPO adduct formation in PB-induced microsomes. DMPO adduct formation was measured by ESR under aerobic conditions, as described in Materials and Methods. The ESR spectrum indicates the presence of DMPO-OOH (*spectrum A*) and DMPO-OH (*spectrum B*) adducts. In control incubations without microsomes (*spectrum C*) or without NADPH (*spectrum D*), no DMPO adduct could be detected. Representative experiments of three are shown. ESR settings were the same as described in the legend to Fig. 3.

The observation that βNF microsomes were able to stimulate ADR-induced $H_2O_2$ formation to a similar extent as were PB microsomes may indicate other routes of molecular oxygen reduction by ADR in βNF microsomes. Presently, we cannot exclude the possibility of other CYP-mediated reduction reactions in βNF microsomes.

**ADR-induced hydroxyl radical formation and LPO.** Aerobic incubation of ADR with PB microsomes, NADPH, and DMPO also gave rise to an ESR signal for a DMPO-OH radical adduct (Fig. 5, *spectrum B*) similar to that reported for the hydroxyl radical adduct of DMPO (44). Hydroxyl radicals have been shown to initiate membrane LPO (15). ADR (100 μM) was found to produce a significant time-dependent increase in LPO in both PB and βNF microsomes (Fig. 8). Whereas superoxide dismutase (40 μg/ml) was shown not to inhibit ADR-stimulated LPO in these microsomal incubations (Table 2), DMU (a hydroxyl radical scavenger) was nearly 100% effective as an inhibitor (Table 2), indicating that hydroxyl radicals were involved in the ADR-induced LPO. Importantly, DMU had no effect on RED activity and did not inhibit aminopyrine *N*-demethylase activity (15). This indicates that inhibition of CYP activity by DMU is not likely.

Inasmuch as SK&F 525-A interfered with the LPO assay (data not shown), experiments with CYP inhibitors were performed only with MP, EN, and EP. MP inhibited ADR-stim-

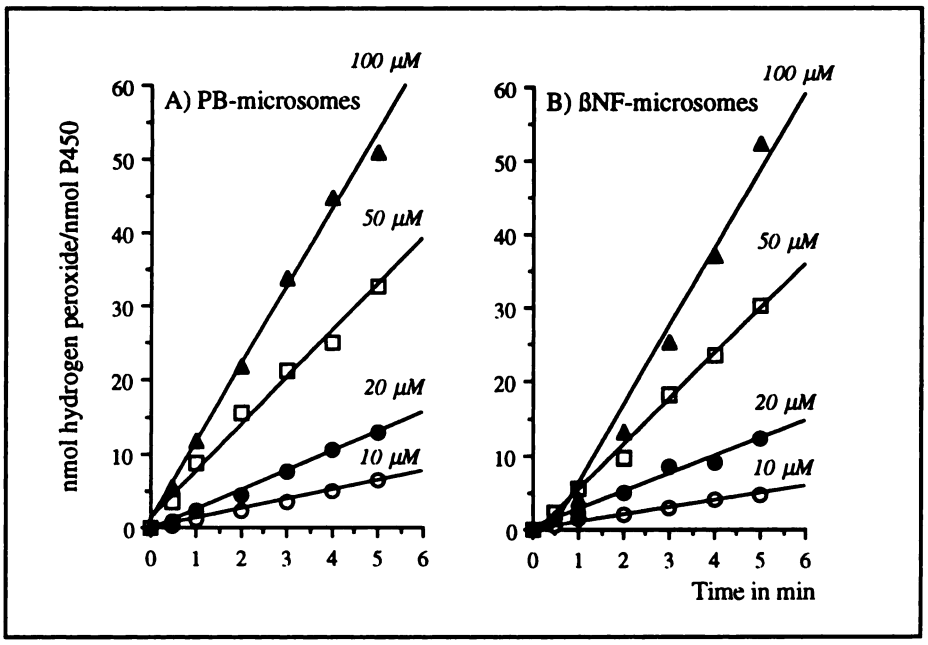


**Fig. 6.** Hydrogen peroxide formation in rat liver microsomes under aerobic conditions. ADR-induced hydrogen peroxide formation was determined in PB microsomes (A) and βNF microsomes (B). The incubation mixture contained microsomes (1 mg/ml protein), 5 mM $MgCl_2$, 50 mM methanol, 3000 mU/ml catalase, 5 mM semicarbazide, 0.5 mM NADP, 1 unit/ml glucose-6-phosphate dehydrogenase, and 5 mM glucose-6-phosphate, in 50 mM Tris·HCl buffer, pH 7.4, containing 0.1 mM DTPA. The final concentration of ADR ranged from 10 to 100 µM. Values shown were corrected for endogenous hydrogen peroxide formation (see text) and represent the mean of three experiments.

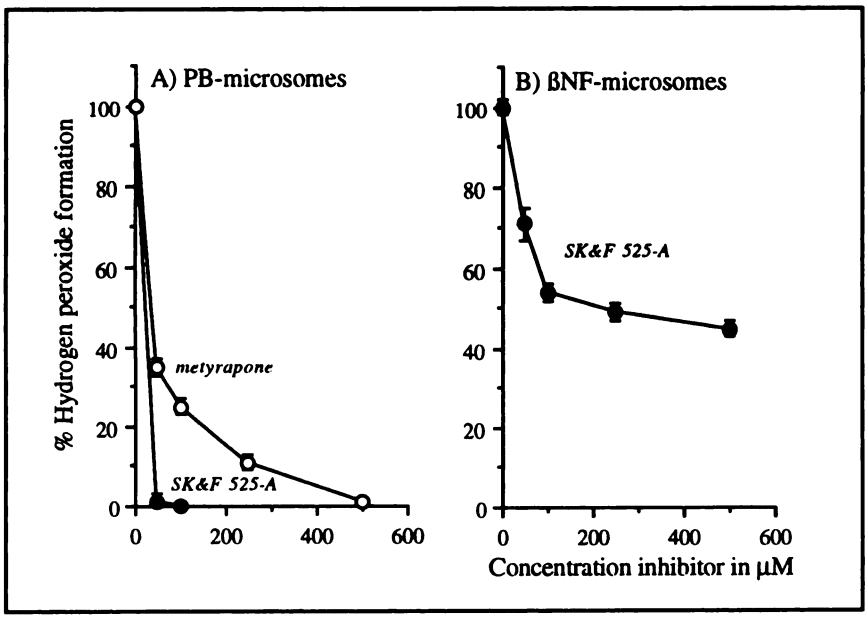


**Fig. 7.** Inhibitory effects of SK&F 525-A and MP on ADR-induced hydrogen peroxide formation in different microsomal fractions of rat liver. ADR (50 µM) was incubated for 10 min at 37° with different concentrations of SK&F 525-A and MP in PB-induced microsomes (A) and βNF-induced microsomes (B). The results (corrected for endogenous hydrogen peroxide formation) are expressed as percentage of the means ± standard deviations of three experiments.

ulated LPO by 40% with PB microsomes (Table 2), whereas only a slight inhibition (15%) was observed with βNF microsomes (Table 2). Also, EN (10 µM) and EP (10 µM) were rather ineffective in inhibiting ADR-induced LPO with βNF microsomes (Table 2).

**CYP2B1-mediated one-electron reduction of ADR to ADRSQ.** Inasmuch as CYP2B1 is the major PB-inducible CYP isoenzyme in rat liver (27), the ability of CYP2B1 to reduce ADR to ADRSQ was investigated by ESR in reconstituted systems consisting of purified RED and purified CYP2B1. Anaerobic incubation of ADR with a fully reconstituted system of CYP2B1 (70 nM) and RED (70 nM) produced ESR signals for ADRSQ similar to those obtained with PB microsomes (Fig. 3). Incubation of ADR (0.1 mM) with RED (70 nM) alone produced 2-fold weaker ESR signals for ADRSQ, compared with the fully reconstituted system of CYP2B1 and RED. The ESR signal intensity for ADRSQ in the reconstituted system of CYP2B1 and RED was 100 ± 15%, compared with 56 ± 6% with RED alone (three experiments; $p < 0.001$). No ESR signal for ADRSQ was detected in incubation mixtures lacking either RED, NADPH, or ADR (data not shown).

**CYP2B1-mediated reduction of ADR measured by NADPH oxidation.** A convenient measure of the reductive metabolism of ADR is the initial rate of NADPH oxidation under anaerobic conditions (47). In PB microsomes, 22 ± 2 µM NADPH/min (four experiments) was oxidized in the presence of 0.1 mM ADR. SK&F 525-A (50 µM) was able to inhibit ADR-induced NADPH oxidation in PB microsomes by >50% (Table 3). Moreover, incubation of ADR with antibodies against CYP2B1 and CYP2B2 (KO1, from Dr. P. Kremers, Université de Liège, Liège, Belgium) resulted in 65% inhibition of ADR-induced NADPH oxidation (Table 3).

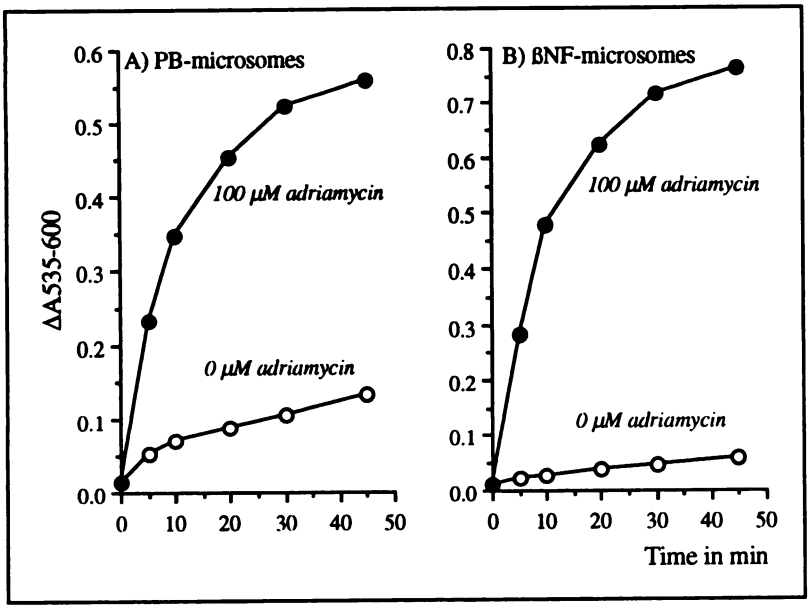


**Fig. 8.** Time course of ADR-stimulated LPO. ADR-induced LPO was investigated with PB-induced (A) and βNF-induced (B) rat liver microsomes, as described in Materials and Methods. Incubation mixtures contained microsomes (1 mg/ml protein), 0.1 mM ADR, 0.1 mM NADP, 1 unit/ml glucose-6-phosphate dehydrogenase, and 5 mM glucose-6-phosphate, in 50 mM Tris·HCl buffer, pH 7.4, containing 150 mM KCl. One representative experiment of three is shown.

**TABLE 2**

**Inhibition by CYP inhibitors of ADR-induced LPO in microsomal incubations**

ADR-induced LPO in PB and βNF microsomes was investigated as described in Materials and Methods. The effects of different CYP inhibitors, superoxide dismutase, and DMU on the LPO reaction were investigated. The formation of TBA-reactive products is expressed as percentage of the results obtained with the complete incubation mixture. The means ± standard deviations of four determinations are shown.

| System | LPO | |
|---|---|---|
| | PB microsomes | βNF microsomes |
| | % | |
| Complete[a] | 100 ± 4 | 100 ± 4 |
| With superoxide dismutase (40 µg/ml) | 97 ± 6 | 97 ± 5 |
| With DMU (0.1 M) | 0 ± 4 | 0 ± 5 |
| With MP (0.05 mM) | 64 ± 4[b] | 97 ± 4 |
| With MP (0.10 mM) | 60 ± 4[b] | 88 ± 3[b] |
| With MP (0.25 mM) | 67 ± 5[b] | 86 ± 3[b] |
| With EN (10 µM) | ND[c] | 79 ± 5[b] |
| With EP (10 µM) | ND | 77 ± 4[b] |

[a] Complete mixtures contained ADR (0.1 mM), NADP (0.1 mM), glucose-6-phosphate (5 mM), glucose-6-phosphate dehydrogenase (1 unit/ml), and microsomes (1 mg/ml protein), in 50 mM Tris·HCl buffer, pH 7.4, containing 150 mM KCl.
[b] $p < 0.001$.
[c] ND, not determined.

**TABLE 3**

**ADR-induced NADPH oxidation and the effects of CYP inhibitors**

ADR-induced NADPH oxidation in PB microsomes and in reconstituted systems of purified CYP2B1 and purified RED was investigated as described in Materials and Methods. Data represent the means ± standard deviations of at least four experiments.

| System | ADR-induced NADPH oxidation | |
|---|---|---|
| | PB microsomes | Reconstituted system |
| | µM/min | |
| Complete | 22.4 ± 2.1[a] | 14.6 ± 1.2[b] |
| Without CYP2B1 | ND[c] | 6.4 ± 0.3 |
| Without RED | ND | <0.5 |
| With SK&F 525-A (50 µM) | 9.8 ± 0.3[d] | 5.6 ± 0.9[d] |
| With KO1 (1/1000) | 7.7 ± 1.0[d] | 4.3 ± 0.4[d] |

[a] Complete mixture contained PB-induced rat liver microsomes (0.7 mg/ml protein), ADR (0.1 mM), and NADPH (1 mM).
[b] Complete mixture contained CYP2B1 (70 nM), RED (70 nM), ADR (0.1 mM), and NADPH (1 mM).
[c] ND, not determined.
[d] $p < 0.001$.

The ability of CYP2B1 to catalyze the one-electron reduction of ADR was also investigated in reconstituted systems of purified CYP2B1 and purified RED. The rate of ADR-induced NADPH oxidation in the presence of RED (70 nM) alone was 2-fold lower than that in a fully reconstituted system of CYP2B1 (70 nM) and RED (70 nM). Addition of SK&F 525-A and KO1 antibody to these incubation mixtures consistently resulted in a strong inhibition of ADR-induced NADPH oxidation (Table 3).

**Relative contributions of CYP2B1 and RED in the reduction of ADR.** Fig. 9 shows that ADR is reduced in a complete reconstituted system of purified CYP2B1 and purified RED, as well as in a system consisting of purified RED alone. In Fig. 9A, the results are shown for incubations of ADR (100 µM) with varying concentrations of RED, reconstituted without (Fig. 9A, *curve 1*) or with (Fig. 9A, *curve 2*) CYP2B1 (70 nM). NADPH oxidation in the absence of ADR was negligible (Fig. 9A). ADR-induced NADPH oxidation slowly increased with increasing concentrations of RED alone, to a maximum of 6.5 ± 0.3 µM/min (Fig. 9A, *curve 1*). In the presence of increasing concentrations of RED and a fixed amount of CYP2B1 (70 nM), the rate of ADR-induced NADPH oxidation rapidly increased to a maximum of 14.6 ± 1.2 µM/min, occurring at equimolar concentrations of CYP2B1 and RED (Fig. 9A, *curve 2*). The results of incubations of ADR with varying amounts of CYP2B1 and a fixed amount of RED (70 nM) are shown in Fig. 9B (*curve 3*). CYP2B1 stimulated the ADR-induced NADPH consumption in a concentration-dependent manner, from 6.5 ± 0.3 to 14.6 ± 1.2 µM/min (three experiments), at a CYP2B1 to RED molar ratio of 1:1.

## Discussion

Despite several studies demonstrating one-electron reductive bioactivation of ADR in the presence of RED (12, 48), NADH

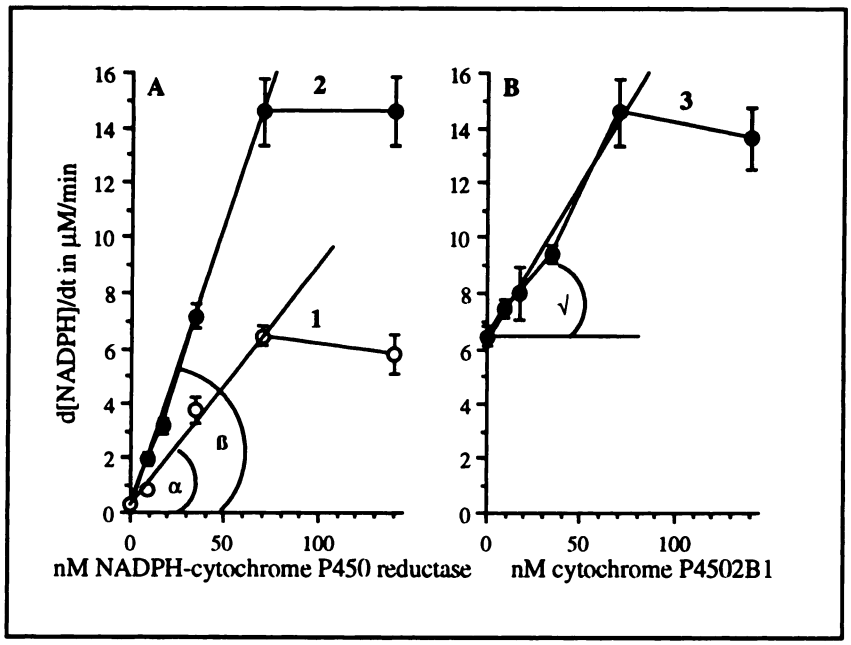


Fig. 9. One-electron reduction of ADR measured as NADPH oxidation in reconstituted systems of purified CYP2B1 and RED. ADR-induced NADPH oxidation was measured as described in Materials and Methods. A, ADR (0.1 mM)-induced NADPH oxidation was measured with varying amounts of RED in the absence (*curve 1*) or presence (*curve 2*) of 70 nM CYP2B1. ○, RED alone; ●, reconstituted system of RED and CYP2B1. B, ADR-induced NADPH oxidation was measured in reconstituted systems with varying amounts of CYP2B1 in the presence of 70 nM RED (*curve 3*). Each value is the mean ± standard deviation of at least three determinations.

dehydrogenase (20), and xanthine oxidase (22), conclusive evidence regarding a possible role of CYP in this one-electron reduction reaction is lacking. It was the main purpose of this investigation to determine the role of CYP in the reductive bioactivation of ADR, relative to the role of RED in this process.

**CYP-mediated one-electron reduction of ADR in liver microsomes.** The present study clearly demonstrates that ADR is a potential substrate for PB-inducible rat liver CYPs. The reverse type I character of the difference spectra (Fig. 1) of ADR with PB microsomes and the inhibitory effect of ADR on CYP-mediated *N*-demethylation of aminopyrine (Fig. 2) indicate binding of ADR to the catalytic site of CYP in this microsomal system. In agreement with previous work showing that PB-inducible CYPs preferentially catalyze the reductive metabolism of TMQ (28), MMC (26), halothane (5), and carbon tetrachloride (4), rates of ADR reduction were greater under anaerobic conditions with PB microsomes, compared with βNF microsomes (Fig. 3). The fact that ADRSQ was formed reductively by CYP in PB microsomes could be definitively concluded from ESR and inhibition studies using SK&F 525-A and MP (Fig. 4; Table 1). These CYP inhibitors inhibited ADR-induced $H_2O_2$ formation in PB microsomes as well (Fig. 7A), indicating a substantial role of PB-inducible CYPs in the microsomal reductive bioactivation of ADR, a process that was previously attributed exclusively to RED (48).

**Contributions of CYP2B1 and RED in the reduction of ADR.** The present study also indicated a role of CYP2B1 (the major PB-inducible isoenzyme of CYP) (27) in the one-electron reduction of ADR to ADRSQ under anaerobic conditions (Fig. 9; Tables 1 and 3). In support of this, incubation of ADR with a complete reconstituted system of purified CYP2B1 and purified RED showed 2-fold stronger ESR signals for ADRSQ than did a system with purified RED alone (Table 1). The strong inhibition of ADR-induced NADPH oxidation by SK&F 525-A and KO1 (an anti-CYP2B1 and anti-CYP2B2 antibody) in reconstituted systems of purified CYP2B1 and purified RED (Table 3) is also consistent with a major role of CYP2B1 in this one-electron reduction reaction of ADR.

In agreement with previous work with TMQ (28, 29), we found that RED alone was able to reduce ADR. RED reduced ADR at an initial rate of 93 nmol of NADPH/nmol of RED/min in the absence of CYP2B1 (Fig. 9, slope α). In the presence of CYP2B1 the initial rate of ADR reduction by RED increased to 204 nmol of NADPH/nmol of RED/min (Fig. 9A, slope β). Thus, the ADR-induced NADPH oxidation by RED occurred at a 2-fold greater rate in the presence of CYP2B1 than in the absence of CYP2B1. Experiments with increasing amounts of CYP2B1 and a fixed amount of RED (70 nM) also showed increased rates of NADPH oxidation (Fig. 9B). The relative contribution of CYP2B1 to the reduction of ADR, calculated from slope √ (Fig. 9B), was 115 nmol of NADPH/nmol of CYP2B1/min. Interestingly, a similar contribution was obtained with RED alone (Fig. 9A, slope α). Thus, this study for the first time clearly demonstrates that reconstituted CYP2B1 contributes to a similar extent as does RED alone to the one-electron reduction of ADR under anaerobic conditions. The results obtained in the present study suggest that reductive bioactivation of ADR by CYP (notably CYP2B1) may have serious consequences for the antitumor efficacy and spectrum of cytotoxicity of this anticancer drug in normal and/or tumor cells with CYP expression.

**Proposed mechanism of ADR reduction by CYP.** All present experiments performed with an equimolar ratio of purified CYP2B1 and purified RED (using both ESR and NADPH oxidation assays) consistently resulted in a 2-fold enhancement of ADR reduction by CYP2B1, compared with RED alone. Although optimal ratios of CYP and RED in reconstituted systems are usually determined empirically, the fact that a 1:1 stoichiometry of RED and CYP2B1 (Fig. 9) caused maximal reduction of ADR indicates that CYP2B1 and RED probably act in concert during the one-electron reduction of ADR to ADRSQ (Fig. 10). If they did not, the effects on ADR reduction would have increased with increasing concen-

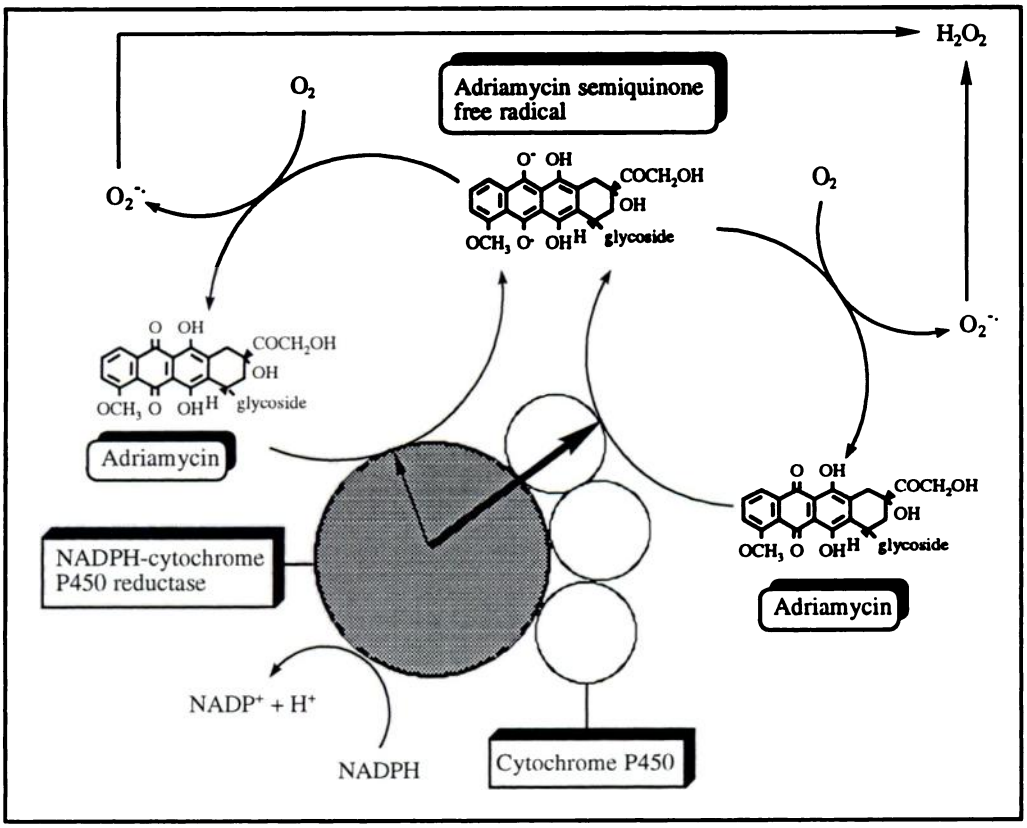


**Fig. 10.** One-electron reductive bioactivation of ADR. Under anaerobic conditions one-electron reduction of ADR by the CYP system results in the formation of ADRSQ. In the presence of molecular oxygen ADRSQ is reoxidized, with concomitant reduction of molecular oxygen, leading to the formation of superoxide anion radicals and hydrogen peroxide.

trations of either RED or CYP2B1, independently of their ratio.

An important factor determining the rate of enzymatic reduction of quinones is the one-electron reduction potential. The one-electron reduction potential for ADR is approximately −300 mV (49). Values in this range are relatively low, which may explain why the rate of reduction of ADR by RED alone is half that of the fully reconstituted system with purified CYP2B1 and RED (Fig. 9). The high affinity binding of ADR to the catalytic site of rat liver CYP (Fig. 1) and the inhibition of CYP2B activity by ADR (Fig. 2) indicate that ADR is a potential substrate for CYP-mediated one-electron reductive bioactivation. Thus, the general concept is that CYP binds ADR to form a CYP-ADR complex, which interacts with RED. Such an arrangement would make ADR-bound CYP more likely to accept electrons from RED, thus leading to an enhanced one-electron reduction of ADR to ADRSQ via CYP (Fig. 10). In fact, substrate binding to CYP has been shown to enhance both the rate of association and the affinity of RED for the preformed CYP-substrate complexes (50). An interesting feature of the proposed mechanism for ADR reduction by CYP is that it closely resembles the mechanism of CYP-mediated one-electron reduction reactions of TMQ (28, 29), NAPQI, and 3,5-dimethyl-NAPQI (9).

**CYP-mediated reductive bioactivation of ADR under aerobic conditions.** Under aerobic conditions, ADRSQ formation from ADR was diminished (Fig. 3, *spectrum F*) and concomitant reduction of molecular oxygen, leading to the formation of $O_2^{\cdot-}$ (Fig. 5, *spectrum A*), $H_2O_2$ (Fig. 6), and ·OH (Fig. 5, *spectrum B*), occurred instead. Studies using MP and SK&F 525-A as potent CYP inhibitors have shown that ADR-induced $H_2O_2$ formation is primarily CYP dependent (Fig. 7). These results suggest that CYP-mediated one-electron reduction of ADR to ADRSQ, followed by ADRSQ autooxidation under aerobic conditions, may constitute the major source for oxygen free radical generation (Fig. 10).

However, apart from redox cycling, molecular oxygen reduction could also result directly from the oxygen reductase activity of CYP. Quinoneimines such as NAPQI and 3,5-dimethyl-NAPQI (9) and the model quinone TMQ (29) have been shown to stimulate oxygen reduction by CYP, with concomitant formation of $H_2O_2$ and ·OH. To what extent binding of ADR to the catalytic site of CYP results in stimulation of the oxygen reductase activity of CYP (i.e., by uncoupling of the CYP reaction cycle), compared with oxygen reduction by redox cycling of the ADR/ADRSQ couple, remains a matter of speculation. For instance, whereas ADR-induced $H_2O_2$ formation was completely inhibited by SK&F 525-A and MP (Fig. 7A) under aerobic conditions, only partial inhibition of ADRSQ formation (as measured by ESR) was observed with these CYP inhibitors under anaerobic conditions (Fig. 4; Table 1) in PB microsomes. Thus, in addition to oxygen reduction due to redox cycling of ADR under aerobic condition, $H_2O_2$ might also have originated independently from the oxygen reductase activity of microsomal CYP.

**Biological consequences of CYP-mediated one-electron reduction of ADR.** The CYP-mediated redox metabolism of ADR and/or the ADR-induced uncoupling of CYP also gave rise to ·OH formation (Fig. 5, *spectrum B*) and caused oxidation of polyunsaturated fatty acids (Table 2). LPO is known to cause irreversible modifications of membrane structure and function (13). In addition, LPO can also liberate aldehydes and other metabolites that cause DNA damage (51) and/or can affect viability and replication of tumor cells (52).

Thus, in addition to the implications for CYP-mediated redox cycling of ADR, our findings (Table 2) suggest a potential toxicological effect associated with ADR reduction by CYP.

Presently, it is not known what effect one-electron reductive bioactivation of quinones by CYP would have on the cytotoxicity and/or antitumor activity of these compounds in cells expressing this enzyme. Unfortunately, the involvement of CYP in the reductive metabolism of cytostatic quinones is not appreciated, because proliferating cells in culture often do not express this hemoprotein or express it at very low concentrations (53). Recently, V79 Chinese hamster cells were genetically engineered to express specific rat liver CYP2B1 and CYP1A1 enzymes (53). Comparative studies on the role of CYP-mediated reductive bioactivation of ADR and MMC in these genetically engineered V79 cells and in freshly isolated rat hepatocytes should be most informative.

**Conclusion.** This study with rat liver microsomes and reconstituted systems of purified CYP2B1 and purified RED demonstrated that rat liver microsomal CYP, and more specifically CYP2B1, catalyzes the one-electron reduction of ADR, in addition to RED. Moreover, rat liver CYP contributes substantially to the generation of radical species causing LPO. Obviously, this newly recognized role of CYP in the one-electron reduction of ADR may have important consequences for the cytotoxicity and/or antitumor activity of this type of quinone anticancer drugs.

#### Acknowledgments

The authors thank Dr. P. Kremers (Université de Liège, Liège, Belgium) for providing the KO1 antibody and Dr. W. L. Alworth (Tulane University, New Orleans, LA) for providing EN and EP.

#### References

1. Murray, M., and G. F. Reidy. Selectivity in the inhibition of mammalian cytochrome P450 by chemical agents. *Pharmacol. Rev.* **42**:85–101 (1990).
2. Potter, D. W., and D. J. Reed. Involvement of FMN and phenobarbital cytochrome P450 in stimulating a one-electron reductive denitrosation of 1-(2-chloroethyl)-3-(cyclohexyl)-1-nitrosourea catalyzed by NADPH-cytochrome P450 reductase. *J. Biol. Chem.* **258**:6906–6911 (1983).
3. Koymans, L., J. H. van Lenthe, R. van de Straat, G. M. Donné-Op den Kelder, and N. P. E. Vermeulen. A theoretical study on the metabolic activation of paracetamol by cytochrome P450: indications for a uniform oxidation mechanism. *Chem. Res. Toxicol.* **2**:60–66 (1989).
4. De Groot, H., and H. Sies. Cytochrome P450, reductive metabolism, and cell injury. *Drug Metab. Rev.* **20**:275–284 (1989).
5. Ahr, H. J., L. J. King, W. Nastainczyk, and V. Ullrich. The mechanism of reductive dehalogenation of halothane by liver cytochrome P450. *Biochem. Pharmacol.* **31**:383–390 (1982).
6. Harrelson, W. G., and R. P. Mason. Microsomal reduction of gentian violet. *Mol. Pharmacol.* **22**:239–242 (1982).
7. Harada, N., and T. Omura. Participation of cytochrome P-450 in the reduction of nitro compounds by rat liver microsomes. *J. Biochem. (Tokyo)* **87**:1539–1554 (1980).
8. Zbaida, S., and W. G. Levine. Role of electronic factors in binding and reduction of azo dyes by hepatic microsomes. *J. Pharmacol. Exp. Ther.* **260**:554–561 (1992).
9. van de Straat, R., J. de Vries, and N. P. E. Vermeulen. Role of hepatic microsomal and purified cytochrome P450 in the one-electron reduction of the quinoneimines and concomitant reduction of molecular oxygen. *Biochem. Pharmacol.* **36**:613–620 (1987).
10. Chesis, P. L., D. E. Levin, M. T. Smith, L. Ernster, and B. N. Ames. Mutagenicity of quinones: pathways of metabolic activation and detoxification. *Proc. Natl. Acad. Sci. USA* **81**:1696–1700 (1984).
11. Weiner, L. M., N. P. Gritzan, N. M. Bazhin, and V. V. Lyakhovich. Microsomal and photochemical oxidation and reduction of 1-piperidinoanthraquinone. *Biochim. Biophys. Acta* **714**:234–242 (1982).
12. Powis, G. Free radical formation by anticancer quinones. *Free Radicals Biol. Med.* **6**:63–101 (1989).
13. Odom, A. L., C. A. Hatwig, J. S. Stanley, and A. M. Benson. Biochemical determinants of Adriamycin toxicity in mouse liver, heart and intestine. *Biochem. Pharmacol.* **43**:831–836 (1992).
14. Bertolatus, J. A., D. Klinzman, D. A. Bronsema, L. Ridnour, and L. W. Oberley. Evaluation of the role of reactive oxygen species in doxorubicin hydrochloride nephrosis. *J. Lab. Clin. Med.* **118**:435–445 (1991).
15. Mimnaugh, E. G., M. A. Trush, and T. E. Gram. Stimulation by Adriamycin of rat heart and liver microsomal NADPH-dependent lipid peroxidation. *Biochem. Pharmacol.* **30**:2797–2804 (1981).
16. Bachur, N. R., S. L. Gordon, M. V. Gee, and H. Kon. NADPH cytochrome P-450 reductase activation of quinone anticancer agents to free radicals. *Proc. Natl. Acad. Sci. USA* **76**:954–957 (1979).
17. Kalyanaraman, B., E. Perez-Reyes, and R. P. Mason. Spin-trapping and direct electron spin resonance investigations of the redox metabolism of quinone anticancer drug. *Biochim. Biophys. Acta* **630**:119–130 (1980).
18. Doroshow, J. H., and K. J. A. Davies. Redox cycling of anthracyclines by cardiac mitochondria. *J. Biol. Chem.* **261**:3068–3074 (1986).
19. Bustamante, J., M. Galleano, E. E. Medrano, and A. Boveris. Adriamycin effects on hydroperoxide metabolism and growth of human breast tumor cells. *Breast Cancer Res. Treat.* **17**:145–153 (1990).
20. Kukielka, E., and A. I. Cederbaum. NADPH- and NADH-dependent oxygen radical generation by rat liver nuclei in the presence of redox cycling agents and iron. *Arch. Biochem. Biophys.* **283**:326–333 (1990).
21. Doroshow, J. H. Role of hydrogen peroxide and hydroxyl radical formation in the killing of Ehrlich tumor cells by anticancer quinones. *Proc. Natl. Acad. Sci. USA* **83**:4514–4518 (1986).
22. Kalyanaraman, B., K. M. Morehouse, and R. P. Mason. An electron paramagnetic resonance study of the interactions between the Adriamycin semiquinone, hydrogen peroxide, iron-chelators, and radical scavengers. *Arch. Biochem. Biophys.* **286**:164–170 (1991).
23. Rumyantseva, G. V., L. M. Weiner, E. I. Frolova, and O. S. Fedorova. Hydroxyl radical generation and DNA strand scission mediated by natural anticancer and synthetic quinones. *FEBS Lett.* **242**:397–400 (1989).
24. Bast, A., and G. R. M. M. Haenen. Cytochrome P450 and glutathione: what is the significance of their interrelationship in lipid peroxidation? *Trends Pharmacol. Sci.* **510**:10–513 (1984).
25. Kennedy, K. A., S. G. Sligar, L. Polomski, and A. C. Sartorelli. Metabolic activation of mitomycin C by liver microsomes and nuclei. *Biochem. Pharmacol.* **31**:2011–2016 (1982).
26. Vromans, R. M., R. van de Straat, M. Groeneveld, and N. P. E. Vermeulen. One-electron reduction of mitomycin C by rat liver: role of cytochrome P450 and NADPH-cytochrome P-450 reductase. *Xenobiotica* **20**:967–978 (1990).
27. Waxman, D. J., and L. Azaroff. Phenobarbital induction of cytochrome P-450 gene expression. *Biochem. J.* **281**:577–592 (1992).
28. Goeptar, A. R., J. M. te Koppele, J. M. S. van Maanen, C. E. M. Zoetemelk, and N. P. E. Vermeulen. One-electron reductive bioactivation of 2,3,5,6-tetramethylbenzoquinone by cytochrome P450. *Biochem. Pharmacol.* **43**:343–352 (1992).
29. Goeptar, A. R., J. M. te Koppele, E. P. A. Neve, and N. P. E. Vermeulen. Reductase and oxidase activity of rat liver cytochrome P450 with 2,3,5,6-tetramethylbenzoquinone as substrate. *Chem.-Biol. Interact.* **83**:249–269 (1992).
30. Lake, B. G. Preparation and characterization of microsomal fractions for studies on xenobiotic metabolism, in *Biochemical Toxicology* (K. Snell and B. Mullock, eds.). IRL Press, Washington DC, 183–191 (1987).
31. Jefcoate, C. R. Measurement of substrate and inhibitor binding to microsomal cytochrome P-450 by optical difference spectroscopy. *Methods Enzymol.* **52**:258–279 (1978).
32. Guengerich, F. P., and M. V. Martin. Purification of cytochrome P-450 NADPH-cytochrome P-450 reductase and epoxide hydratase for a single preparation of rat liver microsomes. *Arch. Biochem. Biophys.* **205**:365–379 (1980).
33. Omura, T., and R. Sato. The carbon monoxide-binding pigment of liver microsomes. *J. Biol. Chem.* **239**:2370–2378 (1964).
34. Vermillon, J. C., and M. J. Coon. Identification of the high and low potential flavins of liver microsomal NADPH-cytochrome P-450 reductase. *J. Biol. Chem.* **253**:2694–2704 (1978).
35. Faeder, E. J., and L. M. Siegel. A rapid micromethod for the determination of FMN and FAD in mixtures. *Anal. Biochem.* **53**:332–336 (1973).
36. Lowry, O. H., N. J. Rosebrough, A. L. Farr, and R. J. Randall. Protein measurement with the Folin phenol reagent. *J. Biol. Chem.* **193**:265–275 (1951).
37. Nash, T. The colorimetric estimation of formaldehyde by means of the Hantzsch reaction. *Biochem. J.* **55**:416–421 (1954).
38. Hildebrandt, A. G., G. Heinemeyer, and I. Roots. Stoichiometric cooperation of NADPH and hexobarbital in hepatic microsomes during the catalysis of hydrogen peroxide formation. *Arch. Biochem. Biophys.* **216**:455–465 (1982).
39. Englander, S. W., D. B. Calhoun, and J. J. Englander. Biochemistry without oxygen. *Anal. Biochem.* **161**:300–306 (1987).
40. Ollinger, K., G. D. Buffington, L. Ernster, and E. Cadenas. Effect of superoxide dismutase on the autooxidation of substituted hydro- and semi-naphthoquinones. *Chem.-Biol. Interact.* **73**:53–76 (1990).
41. Haenen, G. R. M. M., and A. Bast. Protection against lipid peroxidation by a microsomal glutathione-dependent labile factor. *FEBS Lett.* **159**:24–28 (1983).
42. Schenkman, J. B., S. G. Sligar, and D. L. Cinti. Substrate interaction with cytochrome P450, in *Hepatic Cytochrome P450 Monooxygenase System* (J. B. Schenkman and D. Kupfer, eds.). Pergamon Press, Oxford, UK, 587–616 (1982).

43. Testa, B., and P. Jenner. Inhibitors of cytochrome P-450s and their mechanism of action. *Drug Metab. Rev.* **12**:1–117 (1981).
44. Mottely, C., H. D. Connor, and R. P. Mason. [$^{17}$O]Oxygen hyperfine structure for the hydroxyl and superoxide radical adducts of the spin traps DMPO, PBN and 4-POBN. *Biochem. Biophys. Res. Commun.* **141**:622–628 (1986).
45. Hammons, G. J., W. L. Alworth, N. E. Hopkins, F. P. Guengerich, and F. F. Kadlubar. 2-Ethynylnaphthalene as a mechanism based inactivation of cytochrome P-450 catalysed *N*-oxidation of 2-naphthylamines. *Chem. Res. Toxicol.* **2**:367–374 (1989).
46. Gan, L. S. L., A. L. Acebo, and W. L. Alworth. 1-Ethynylpyrene, a suicide inhibitor of cytochrome P-450 dependent benzo(*a*)pyrene hydroxylase activity in liver microsomes. *Biochemistry* **23**:3827–3836 (1984).
47. Minotti, G. NADPH- and Adriamycin-dependent microsomal release of iron and lipid peroxidation. *Arch. Biochem. Biophys.* **277**:268–276 (1990).
48. Bachur, N. R., S. L. Gordon, and M. V. Gee. A general mechanism for microsomal activation of quinone anticancer agents to free radicals. *Cancer Res.* **38**:1745–1750 (1978).
49. Svingen, B. A., and G. Powis. Pulse radiolysis studies on antitumor quinones: radical lifetimes: reactivity with oxygen and one-electron reduction potentials. *Arch. Biochem. Biophys.* **209**:119–126 (1981).
50. Beckes, W. L., and C. S. Eyer. Cytochrome P-450LM2 reduction: substrate effects on the rate of reductase-LM2 association. *J. Biol. Chem.* **264**:6252–6259 (1989).
51. Hruszkewycz, A. M. Evidence for mitochondrial DNA damage by lipid peroxidation. *Biochem. Biophys. Res. Commun.* **153**:191–197 (1988).
52. Hauptlorenz, S., H. Esterbauer, W. Mol, R. Pumpoll, E. Schauenstein, and B. Puschendorf. Effects of the lipid peroxidation product 4-hydroxynonenal and related aldehyde on proliferation and viability of cultured Ehrlich ascites tumor cells. *Biochem. Pharmacol.* **34**:3803–3809 (1985).
53. Glatt, H. R., I. Gemperlein, G. Turchi, H. Heinritz, J. Doehmer, and F. Oesch. Search for cell culture systems with diverse xenobiotic-metabolizing activities and their use in toxicological studies. *Mol. Toxicol.* **1**:313–334 (1987).

**Send reprint requests to:** Nico P. E. Vermeulen, Leiden/Amsterdam Center for Drug Research, Department of Pharmacochemistry, Division of Molecular Toxicology, Vrije Universiteit, De Boelelaan 1083, 1081 HV Amsterdam, The Netherlands.